pH-dependent assembly of 0D to 3D Keggin-based coordination polymers: Structures and catalytic properties†

Fan Yu,‡ Xiang-Jian Kong,‡ Yun-Yun Zheng, Yan-Ping Ren, La-Sheng Long,* Rong-Bin Huang and Lan-Sun Zheng

Received 15th June 2009, Accepted 1st September 2009
First published as an Advance Article on the web 18th September 2009
DOI: 10.1039/b911606k

Four Keggin-based coordination polymers, namely, $\{[Cu_2(4,4'\text{-bpy})(4,4'\text{-Hbpy})_4(H_2O)_4]\text{-}(SiW_{12}O_{40})_2(H_2O)_4\}_n$ (**1**), $\{[Cu_2(4,4'\text{-bpy})(4,4'\text{-Hbpy})_6(SiW_{12}O_{40})_3](4,4'\text{-Hbpy})_2(H_2O)_7\}_n$ (**2**), $\{[Cu_2(\mu_2\text{-}H_2O)_2(4,4'\text{-bpy})_3(SiW_{12}O_{40})](H_2O)_6\}_n$ (**3**) and $\{[Cu_2(\mu_2\text{-OH})(4,4'\text{-bpy})_3(SiW_{12}O_{40})(H_2O)][Cu_2(\mu_2\text{-O})(4,4'\text{-bpy})_4(H_2O)_2]_{0.5}\cdot(H_2O)_3\}_n$ (**4**) (4,4′-bpy = 4,4′-bipyridine) were prepared through the hydrothermal reaction of silicotungstic acid, copper(II) nitrate and 4,4′-bipyridine under different pH conditions. Coordination polymers **1** and **2**, which exhibit 0D and 1D structures respectively, were prepared at pH = 3.5. At pH = 5.5, a 2D coordination polymer **3** was obtained. Increasing the pH of the reaction to 8.5 led to a 3D coordination polymer **4**. The structural diversities of **1–4** reveal that the pH value of the reaction plays a key role in the assembly of POM-based coordination polymers. Investigation of the catalytic properties of **1–4** for the oxidation of ethylbenzene indicates that the catalytic activity of the coordination polymers is closely related to the protonated extent of 4,4′-bpy in the coordination polymers.

Introduction

Although possessing many advantageous properties and regarded as promising green catalysts,[1-3] the use of polyoxometalates (POMs) themselves as heterogeneous catalysts is limited due to the conglomeration and deactivation of POMs in the catalytic process.[4] One of the efficient approaches to overcome such drawbacks is to introduce the POMs into the metal–organic units.[5-10] So far, a great many POM-based coordination polymers with structural diversity have successfully been assembled on the basis of these approaches.[5-10] However, the investigation of the catalytic properties of these materials remains scarce,[11-12] despite the fact that such an investigation is fundamentally important for our understanding of the structure–activity correlations of the POM-based coordination polymers, as well as our rational design of highly efficient POMs-based catalysts.

In previous work, we have demonstrated that the relatively weak coordination ability and large number of terminal and bridge oxygen atoms of the POM anion would result in the assembly of POM-based coordination polymers very sensitive to synthesis conditions.[13-14] Although a kind of weakness from the viewpoint of synthesis, such an inherent property of the POM anion often leads to POM-based coordination polymers exhibiting structural diversity, which provides for the possibility of understanding the structure–activity correlations of the POM-based coordination polymers. Here we report the syntheses, crystal structures and catalytic behaviors of four Keggin-based coordination polymers, namely, $\{[Cu_2(4,4'\text{-bpy})(4,4'\text{-Hbpy})_4(H_2O)_4](SiW_{12}O_{40})_2(H_2O)_4\}_n$ (**1**), $\{[Cu_2(4,4'\text{-bpy})(4,4'\text{-Hbpy})_6(SiW_{12}O_{40})_3](4,4'\text{-Hbpy})_2(H_2O)_7\}_n$ (**2**), $\{[Cu_2(\mu_2\text{-}H_2O)_2(4,4'\text{-bpy})_3(SiW_{12}O_{40})](H_2O)_6\}_n$ (**3**) and $\{[Cu_2(\mu_2\text{-OH})(4,4'\text{-bpy})_3(SiW_{12}O_{40})(H_2O)][Cu_2(\mu_2\text{-O})(4,4'\text{-bpy})_4(H_2O)_2]_{0.5}(H_2O)_3\}_n$ (**4**). Their structural diversities show that the pH value plays a key role in the assembly of POM-based coordination polymers. Investigation of the catalytic properties of the coordination polymers on the oxidation of ethylbenzene reveals that their catalytic activities for the oxidation of ethylbenzene are closely related to the protonated extent of 4,4′-bpy in the coordination polymers.

Experimental

Materials and methods

All reagents used were commercially available and were used as received. The hydrothermal syntheses were carried out in polytetrafluoroethylene lined stainless steel containers under autogenous pressure. The infrared spectra were recorded on a Nicolet AVATAR FT-IR360 Spectrophotometer with pressed KBr pellets. Atomic absorption results were obtained on a Thermo Electron IRIS Intrepid II XSP. TGA curves were prepared on a SDT Q600 Thermal Analyzer. The X-ray powder diffractometry (XRD) was performed with a Panalytical X-Pert PRO diffractometer with Cu-Kα radiation (λ = 0.15418 nm, 40.0 kV, 30.0 mA). The reaction products of oxidation were determined and analyzed by a GC-920 instrument with a capillary column (30 m × 0.25 mm).

Synthesis

$\{[Cu_2(4,4'\text{-bpy})(4,4'\text{-Hbpy})_4(H_2O)_4](SiW_{12}O_{40})_2(H_2O)_4\}_n$ (1) and $\{[Cu_2(4,4'\text{-bpy})(4,4'\text{-Hbpy})_6(SiW_{12}O_{40})_3](4,4'\text{-Hbpy})_2(H_2O)_7\}_n$ (2). 1.15 g silicotungstic acid ($H_4SiW_{12}O_{40}$, 0.4 mmol), 0.156 g

State Key Laboratory of Physical Chemistry of Solid Surface and Department of Chemistry, College of Chemistry and Chemical Engineering, Xiamen University, Xiamen, 361005, China. E-mail: lslong@xmu.edu.cn

† CCDC reference numbers 736089–736092. For crystallographic data in CIF or other electronic format see DOI: 10.1039/b911606k

‡ The first and second authors have contributed equally to this work.

4,4′-bipyridine (4,4′-bpy, 1.0 mmol) and 0.148 g copper(II) nitrate ($Cu(NO_3)_2{\cdot}6H_2O$, 0.5 mmol) were dissolved in 18 mL water with stirring at room temperature. The pH value was adjusted to about 3.5 by addition of 1.0 mol L^{-1} NaOH. The solution was heated to 180 °C for 50 h and then cooled to 100 °C with a rate of 10 °C h^{-1}. After 16 h, the solution was cooled to room temperature at a rate of 3 °C h^{-1}. Green crystals of **1** (yield 25% based on 4,4′-bpy) and purple crystals of **2** (yield 35% based on 4,4′-bpy) were collected manually. Anal. Calcd for $C_{50}H_{60}N_{10}O_{88}Cu_2Si_2W_{24}$ (**1**): C, 8.83; H, 0.89; N, 2.06; Found: C, 8.54; H, 0.97; N, 1.96; Calcd for $C_{90}H_{94}N_{18}O_{127}Cu_2Si_3W_{36}$ (**2**): C, 10.51; H, 0.92; N, 2.45; Found: C, 10.21; H, 0.98; N, 2.34. IR (KBr, cm^{-1}): 3442.7 s, 2956.0 m, 2924.5 s, 2854.0 m, 1617.4 s, 1489.2 w, 1457.7 w, 1418.3 w, 1383.8 w, 1276.6 w, 1222.3 w, 1075.9 w, 1016.8 m, 972.1 s, 922.0 s, 889.3 w, 791.5 s, 532.7 m for **1**; 3441 s, 3225 w, 3163 w, 3104 w, 2923 w, 2852 w, 1638 m, 1614 w, 1490 m, 1413 m, 1221 w, 1072 m, 1014 m, 976 s, 922 s, 885 m, 796 s, 535 m for **2**.

$\{[Cu_2(\mu_2\text{-}H_2O)_2(4,4'\text{-bpy})_3(SiW_{12}O_{40})](H_2O)_6\}_n$ (3). 0.36 g silicotungstic acid ($H_4SiW_{12}O_{40}$, 0.125 mmol), 0.12 g pyazine (pz, 1.5 mmol), 0.04 g 4,4′-bipyridine (4,4′-bpy, 0.26 mmol) and 0.148 g copper(II) nitrate ($Cu(NO_3)_2{\cdot}6H_2O$, 0.5 mmol) were dissolved in 18 mL water with stirring at room temperature. The pH value was adjusted to about 5.5 by addition of 1.0 mol L^{-1} NaOH. The solution was heated to 180 °C for 50 h and then cooled to 120 °C at a rate of 10 °C h^{-1}. After 16 h, the solution was cooled to room temperature with a rate of 3 °C h^{-1}. Then green crystals of **3** were obtained in 20% yield based on 4,4′-bpy. Anal. Calcd for $C_{30}H_{40}N_6O_{48}Cu_2SiW_{12}$ (**3**): C, 9.97; H, 1.12; N, 2.33; Found: C, 10.07; H, 1.18; N, 2.41. IR (KBr, cm^{-1}): 3448 s, 2923 w, 2852 w, 1610 s, 1560 m, 1415 m, 1221 m, 1103 s, 1062 s, 952 s, 885 s, 811 s, 509 m, 486 m, 477 m.

$\{[Cu_2(\mu_2\text{-}OH)(4,4'\text{-bpy})_3(SiW_{12}O_{40})(H_2O)][Cu_2(\mu_2\text{-}O)(4,4'\text{-bpy})_4(H_2O)_2]_{0.5}(H_2O)_3\}_n$ (4). 1.15 g silicotungstic acid ($H_4SiW_{12}O_{40}$, 0.4 mmol), 0.089 g β-alanine (1.0 mmol), 0.156 g 4,4′-bipyridine (4,4′-bpy, 1.0 mmol) and 0.148 g copper(II) nitrate ($Cu(NO_3)_2{\cdot}6H_2O$, 0.5 mmol) were dissolved in 18 mL water with stirring at room temperature. The pH value was adjusted to about 8.5 by addition of 1.0 mol L^{-1} NaOH. The solution was heated to 160 °C for 24 h and then cooled to room temperature with a rate of 4 °C h^{-1}. The blue club-shaped crystals of **4** were obtained in 30% yield based on 4,4′-bpy. Anal. Calcd for $C_{100}H_{102}N_{20}O_{93}Cu_6Si_2W_{24}$ (**4**): C, 15.16; H, 1.30; N, 3.54; Found: C, 15.06; H, 1.39; N, 3.48. IR (KBr, cm^{-1}): 3444 s, 3099 m, 2924 w, 2853 w, 1610 s, 1536 m, 1492 m, 1416 s, 1221 m, 1070 m, 1008 m, 945 m, 898 s, 806 s, 644 w, 541 w. In fact, **4** could also have been obtained through the hydrothermal reaction at 180 °C for 50 h (as described for **1** to **3**), but the crystals of **4** were too small and the yield was too low.

X-ray crystallography

Data were collected on a Bruker SMART 2000 diffractometer with Mo-Kα radiation at 298 K for **2**, **4**; 223 K for **1** and 123 K for **3**. Absorption corrections were applied using the multi-scan program SADABS.[15] The structures were solved by direct methods, and the non-hydrogen atoms were refined anisotropically by the least-squares method on F^2 using the SHELXTL program.[16] The hydrogen atoms of organic ligand were generated geometrically (C–H = 0.96 Å, N–H = 0.90 Å). Crystal data, as well as details of the data collection and refinement, for **1** to **4** are summarized in Table 1.

Catalytic experiment

Oxidation of ethylbenzene (0.3 mL, 2.44 mmol) was carried out in a 50 mL round bottom flask fitted with a water-cooled condenser, using aqueous 70 wt% t-butylhydroperoxide (TBHP, 0.754 mL, 4.88 mmol) as an oxidant in acetonitrile (8 mL). The catalyst was added into a mixture of ethylbenzene and t-butylhydroperoxide at 343 K. After 12 h, the mixture was centrifuged to remove the catalyst and analyzed by gas chromatography, using a flame-ionization detector (FID) and a capillary column (30 m × 0.25 mm).

Table 1 Crystal data as well as details of data collection and refinement for **1** to **4**

	1	**2**	**3**	**4**
Formula	$C_{50}Cu_2H_{60}N_{10}O_{88}Si_2W_{24}$	$C_{90}Cu_2H_{94}N_{18}O_{127}Si_3W_{36}$	$C_{30}Cu_2H_{40}N_6O_{48}SiW_{12}$	$C_{100}Cu_6H_{102}N_{20}O_{93}Si_2W_{24}$
M_r	6804.74	10289.78	3614.05	7921.84
crystal system	triclinic	triclinic	monoclinic	orthorhombic
Space group	$P\bar{1}$	$P\bar{1}$	$P2_1/n$	$Pbam$
a (Å)	13.129(2)	12.166(2)	13.095(2)	27.022(5)
b (Å)	13.145(2)	17.906(3)	15.757(3)	28.597(5)
c (Å)	17.791(3)	20.973(3)	14.741(3)	11.116(2)
α (deg)	83.983(3)	68.720(2)	90	90
β (deg)	73.094(3)	86.867(3)	94.479(3)	90
γ (deg)	82.909(3)	83.182(3)	90	90
V (Å^3)	2907.5(8)	4227(1)	3032(1)	8590(3)
Z	1	1	2	2
D_c (g cm^3)	3.886	4.042	3.958	3.063
μ (mm^{-1})	24.111	24.757	23.476	16.827
R(int)	0.0767	0.0827	0.0546	0.0631
Data/params	9880/793	14142/1225	5106/457	7797/615
θ (deg)	1.73-25.00	1.23-25.00	1.89-25.00	1.51-25.00
absd reflns	7700	11092	4895	7095
R_1 [$I > 2\sigma(I)$][a]	0.0759	0.0804	0.0904	0.0809
wR_2(all data)[b]	0.1811	0.1772	0.1805	0.1817

[a] $R_1 = \Sigma \, \| F_o | - | F_c \| / \Sigma \, | F_o |$. [b] $wR_2 = \{\Sigma \, [w(F_o^2 - F_c^2)^2] / \Sigma \, [w(F_o^2)^2]\}^{1/2}$.

Assignments were made by comparison with authentic samples analyzed under the same conditions. The oxidation of styrene (0.1 mL, 0.86 mmol) reactions were carried out by adopting the same procedure as described above for the oxidation of ethylbenzene.

Results and discussions

Description of crystal structures

$\{[Cu_2(4,4'\text{-bpy})(4,4'\text{-Hbpy})_4(H_2O)_4]\cdot(SiW_{12}O_{40})_2\cdot(H_2O)_4\}_n$ (1). Crystal structure analysis reveals that the coordination polymer **1** consists of two $SiW_{12}O_{40}^{4-}$ anions, one $[Cu_2(4,4'\text{-bpy})(4,4'\text{-Hbpy})_4(H_2O)_4]^{8+}$ unit and four lattice water molecules. The dinuclear copper unit, $[Cu_2(4,4'\text{-bpy})(4,4'\text{-Hbpy})_4(H_2O)_4]^{8+}$, contains two different but symmetrically equivalent Cu(II) centers, exhibiting an H-shape similar to those of $[Ni_2(4,4'\text{-Hbpy})_4(4,4'\text{-bpy})(H_2O)_6]\cdot(SiW_{12}O_{40})_2\cdot 16H_2O$[13a] as shown in Fig. 1. The Cu(II) ion is five coordinated by two water molecules and three nitrogen atoms from two monoprotonated 4,4′-Hbpy ligands and one bridged 4,4′-bpy ligand, respectively. Each of the 4,4′-Hbpy ligands in both sides of the dinuclear copper units acting as a proton donor is hydrogen-bonded to the $SiW_{12}O_{40}^{4-}$ anion (Fig. 2) (N2···O39 = 2.76 (2) Å, N2···H2B···O39 = 158.8°; N4···O27 = 2.66 (2) Å, N4···H4B···O27 = 157.3°).

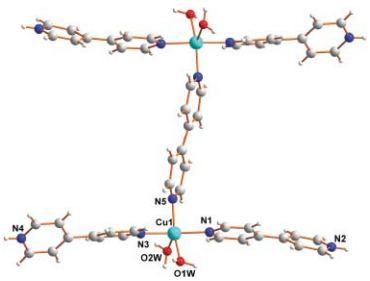

Fig. 1 Ball and stick plot showing the $[Cu_2(4,4'\text{-bpy})(4,4'\text{-Hbpy})_4(H_2O)_4]^{8+}$ unit in **1**.

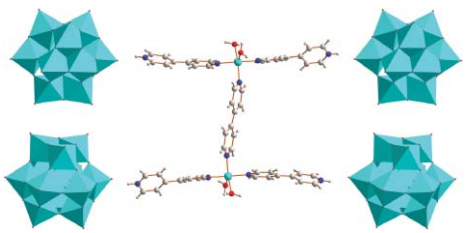

Fig. 2 Plot showing the hydrogen bonding between $SiW_{12}O_{40}^{4-}$ anions and the $[Cu_2(4,4'\text{-bpy})(4,4'\text{-Hbpy})_4(H_2O)_4]^{8+}$ unit in **1**.

$\{[Cu_2(4,4'\text{-bpy})(4,4'\text{-Hbpy})_6(SiW_{12}O_{40})_3](4,4'\text{-Hbpy})_2\ (H_2O)_7\}_n$ (2). Crystal structural analysis reveals that there are two different but symmetrically equivalent Cu(II) centers in **2**. Each Cu(II) ion is six coordinated by two oxygen atoms from $SiW_{12}O_{40}^{4-}$ anions and four nitrogen atoms with three from 4,4′-Hbpy and one from 4,4′-bpy (Fig. 3). The adjacent dinuclear copper units linked by the $SiW_{12}O_{40}^{4-}$ anions, form a "Z"-shaped 1D chain structure (Fig. 4). The 4,4′-Hbpy ligands are hydrogen-bonded to water molecules and $SiW_{12}O_{40}^{4-}$ anions in adjacent chains (N2···O2W = 2.69 (4) Å, N2···H2B···O2W = 147.3°; N4···O3W = 2.68 (5) Å, N4···H2B···O3W = 168.7°, N6···O29 = 3.03 (3) Å, N6···H6B···O29 = 148.1°). The dissociative 4,4′-Hbpy cations are hydrogen-bonded to the coordination water molecules (N8–O1W = 2.78 (4) Å, N8···H8B···O1W = 157.7°; N9···O1WA = 2.70 (8) Å).

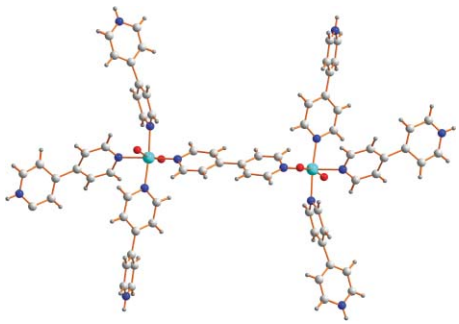

Fig. 3 Ball and stick plot showing the $[Cu_2(4,4'\text{-bpy})(4,4'\text{-Hbpy})_6]^{10+}$ units in **2**.

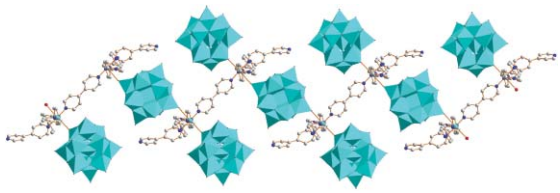

Fig. 4 Plot showing the infinite chain of $[Cu_2(4,4'\text{-bpy})(4,4'\text{-Hbpy})_6(SiW_{12}O_{40})_3]_n^{2n-}$ units in **2**.

$\{[Cu_2(\mu_2\text{-}H_2O)_2(4,4'\text{-bpy})_3(SiW_{12}O_{40})](H_2O)_6\}_n$ (3). Coordination polymer **3** consists of one $[Cu_2(\mu_2\text{-}H_2O)_2(4,4'\text{-bpy})_3]_n^{4n+}$ unit, one $SiW_{12}O_{40}^{4-}$ anion and six guest water molecules. As shown in Fig. 5a, each copper(II) ion in **3** features contributions from six coordinating atoms (two N atoms from two 4,4′-bpy molecules, four oxygen atoms with three from water molecules and one from $SiW_{12}O_{40}^{4-}$ anion). Two Cu(II) ions are bridged by a pair of μ_2-H_2O (Cu···O1W = 1.99 (3) Å, Cu···O1WA = 1.96 (3) Å, Cu1A–O1W–Cu1 = 102.6 (13)°) to form a dinuclear copper unit (Fig. 5a). The adjacent dinuclear units linked by sharing one 4,4′-bpy forms a 1D chain structure of $[Cu_2(\mu_2\text{-}H_2O)_2(4,4'\text{-bpy})_3]_n^{4n+}$ (Fig. 5b), which is further extended into a 2D layer structure of **3** through each $SiW_{12}O_{40}^{4-}$ anion coordinating to two Cu(II) cations respectively from two adjacent 1D chains of $[Cu_2(\mu_2\text{-}H_2O)_2(4,4'\text{-bpy})_3]_n^{4n+}$ (Fig. 6).

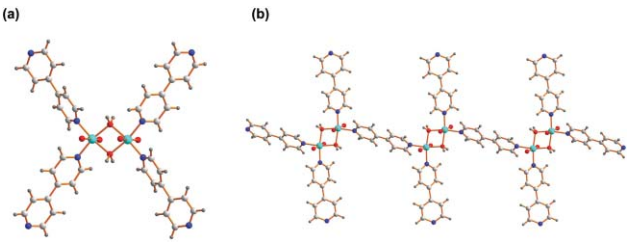

Fig. 5 (a) Stick plot showing the $[Cu_2(4,4'\text{-bpy})_3(\mu_2\text{-}H_2O)_2]^{4+}$ units in **3**; (b) Plot showing the 1D $[Cu_2(\mu_2\text{-}H_2O)_2(4,4'\text{-bpy})_3]_n^{4n+}$ in **3**.

$\{[Cu_2(\mu_2\text{-OH})(4,4'\text{-bpy})_3(SiW_{12}O_{40})][Cu_2(\mu_2\text{-O})(4,4'\text{-bpy})_4(H_2O)_2]_{0.5}(H_2O)_4\}_n$ (4). Crystal structure analysis reveals that

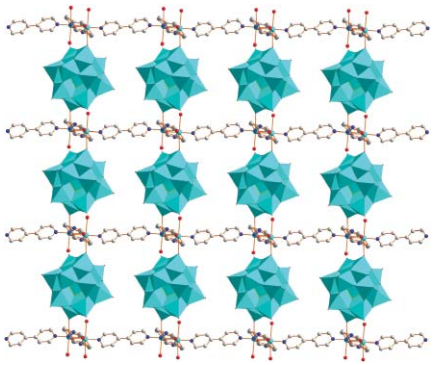

Fig. 6 Plot showing the 2D $[Cu_2(\mu_2\text{-}H_2O)_2(4,4'\text{-bpy})_3(SiW_{12}O_{40})]_n$ in **3** viewed along the *c* axis.

the coordination polymer **4** consists of one $[Cu_2(\mu_2\text{-OH})(4,4'\text{-bpy})_3(SiW_{12}O_{40})]^-$ anion unit, one $[Cu_2(\mu_2\text{-O})(4,4'\text{-bpy})_4(H_2O)_2]^{2+}$ cation unit and water molecules. There are two independent Cu(II) centers in the $[Cu_2(\mu_2\text{-OH})(4,4'\text{-bpy})_3(SiW_{12}O_{40})]^-$ unit (Fig. 7), Cu1 is five coordinated by three N atoms from three 4,4′-bpy ligands, two O atoms with one from $SiW_{12}O_{40}^{4-}$ and another from the μ_2-OH which bridged to Cu2. Cu2 lies in a distorted octahedron geometry center and is six coordinated by three N atoms from three 4,4′-bpy ligands, three O atoms from two $SiW_{12}O_{40}^{4-}$ and one μ_2-OH that bridged Cu1. Cu1 and Cu2 are connected by one μ_2-OH with distances of 1.893(16) Å (Cu1–OH) and 1.936(16) Å (Cu2–OH), and the angle of 131.3 (9)° for Cu2–(μ_2-OH)–Cu1. Cu3 is four coordinated by two nitrogen atoms from three 4,4′-bpy ligands, two O atoms with one from H_2O and one O atom from the μ_2-O which bridged to Cu3A (Cu3–O26 = 1.814 (6) Å, Cu3–O26–Cu3A = 180°). The 3D structure of $[Cu_2(\mu_2\text{-OH})(4,4'\text{-bpy})_3(SiW_{12}O_{40})]_n^{n-}$ anion frameworks can be viewed as a set of parallel 2D cation networks of $[Cu_2(\mu_2\text{-OH})(4,4'\text{-bpy})_3]_n^{3n+}$ (Fig. 8) vertically linked by the $SiW_{12}O_{40}^{4-}$ anions as illustrated in Fig. 9a. The $[Cu_2(\mu_2\text{-O})\ (4,4'\text{-bpy})_4(H_2O)_2]^{2+}$ cation is located in the pore of the 3D anion framework (Fig. 9b).

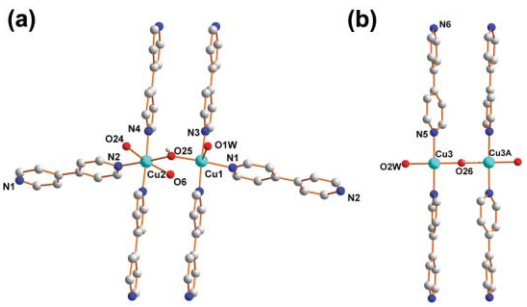

Fig. 7 (a) Ball and stick plot showing the $[Cu_2(\mu_2\text{-OH})(4,4'\text{-bpy})_3]$ unit; (b) ball and stick plot showing the $[Cu_2(\mu_2\text{-O})(4,4'\text{-bpy})_4(H_2O)_2]$ unit in **4**.

pH effect on the structure of Keggin-based coordination polymers

Since coordination polymers **1** to **4** were synthesized from similar modular building units and the main difference in the synthetic conditions is the pH of the reaction, their structural differences are thus related to the pH effect. Based on the structures of **1** to **4**, it was found that the influence of the pH of the reaction on the structures of the coordination polymers is in fact based

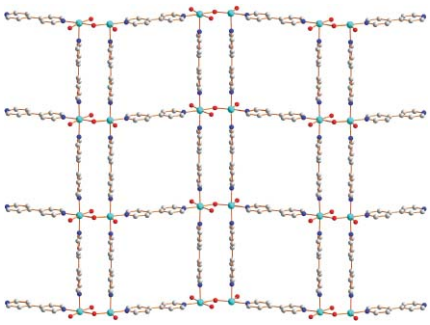

Fig. 8 Plot showing 2D cation network of $[Cu_2(\mu_2\text{-OH})(4,4'\text{-bpy})_3]_n^{3n+}$ viewed along the *b* axis.

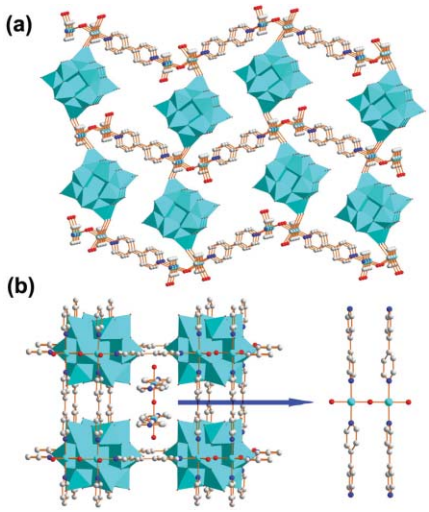

Fig. 9 Plot showing 3D structure of **4** viewed along the *c* axis (a) and along the *b* axis (b).

on the protonation of 4,4′-bpy and the bridge mode of adjacent copper(II) centers. For example, at pH = 3.5, **1** (0D) and **2** (1D) were obtained due to 4,4′-Hbpy being highly protonated; at pH = 5.5 and 8.5, **3** (2D) and **4** (3D) were prepared respectively due to no 4,4′-bpy being protonated. These results indicate that high pH values for the reaction would favor the formation of high dimensional coordination polymers, consistent with previous results.[13a] Notably, in comparison with **1** and **2** in which the adjacent two Cu(II) ions are only bridged by the 4,4′-bpy ligand (Fig. 10a), the adjacent Cu(II) ions in **3** and **4** are additionally bridged with μ_2-H_2O (Cu-(μ_2-H_2O)-Cu) (Fig. 10b) and μ_2-OH

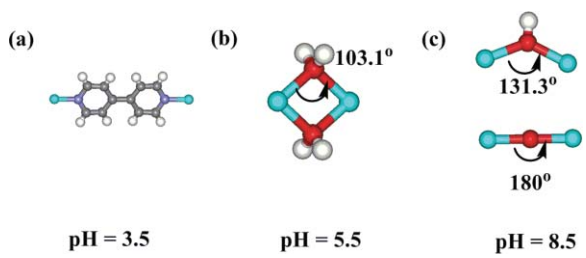

Fig. 10 Plot showing dinuclear copper units, Cu-(4,4′-bpy)-Cu in **1** and **2** (a); Cu-(μ_2-H_2O)$_2$-Cu in **3** (b); Cu-(μ_2-OH)-Cu) and Cu-(μ_2-O)-Cu in **4** (c).

(Cu-(μ_2-OH)-Cu) and μ_2-O (Cu-(μ_2-O)-Cu) (Fig. 10c) respectively, indicating that the high pH value of the reaction favors the formation of hydroxyl and oxygenic bridges.

Thermogravimetric analysis

The thermogravimertric analysis (TGA) for complexes **1** to **4** was performed to illustrate the stability of the polymers. As shown in Fig. 11, the TGA curve for **1** displays an initial weight loss of 0.95% between room temperature and 200 °C, suggesting the loss of water molecules of crystallization (calcd 1.05%). No further weight loss was observed between 200 °C and 300 °C, indicating that the composition of the dehydrated product remains unchanged over this temperature range. The second weight loss of 1.17% covering a temperature range from 300 to 500 °C is very close to the coordination water molecules (calcd 1.05%), indicating the framework of **1** is stable up to 500 °C. At temperatures higher than 500 °C, **1** was rapidly decomposed.

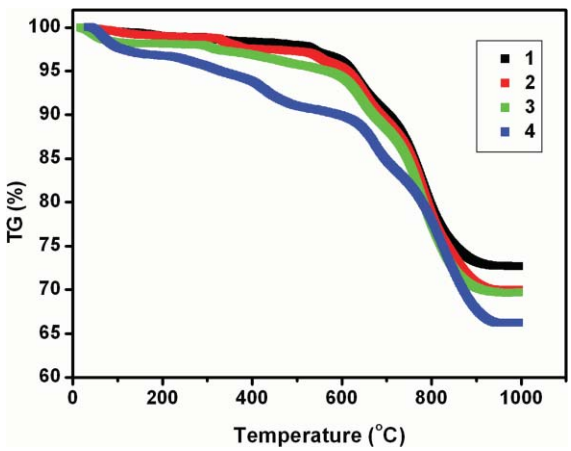

Fig. 11 TGA curve for complexes **1–4** over the temperature 20–1000 °C in a nitrogen-gas atmosphere.

The TGA curves for **2** and **3** show that frameworks of **2** and **3** are stable up to 500 °C, which are very similar to that of **1**. The TGA curve for **4** displays an initial weight loss of 2.31% between room temperature and 100 °C, suggesting the loss of water of crystallization molecules (calcd 2.27%). Between 100 °C and 600 °C, **4** shows a weight loss of 7.81% which is very close to the two 4,4′-bpy molecules (calcd 7.87%).

Catalytic properties

The oxidation of ethylbenzene (Scheme 1) catalyzed by **1** to **4** were performed under the same reaction conditions,[17] so as to reveal the relationship between structure and catalytic properties. Owing to **1** to **4** containing different amounts of $SiW_{12}O_{40}^{4-}$ anions, in order to keep the amount of $SiW_{12}O_{40}^{4-}$ in **1** to **4** unchanged (0.01 mmol), 0.005 mmol **1**, 0.003 mmol **2**, 0.01 mmol **3**, and 0.01 mmol **4** were used for the oxidation of ethylbenzene.

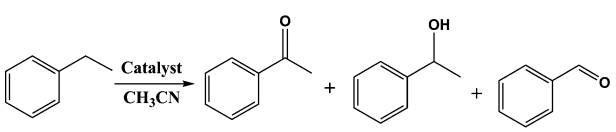

Scheme 1 Oxidation of ethylbenzene to acetophenone.

Table 2 Catalytic activities of **1** to **4** for the oxidation of ethylbenzene

Catalyst	T (K)	Conv (%)[b]	Selec (%)[c]	Yield (%)[d]
1	343	27.6	76.0	20.9
2	343	22.4	75.9	17.0
3	343	51.1	85.2	43.5
4	343	44.3	82.0	36.3
Blank	343	6.6	—	—

[a] Ethylbenzene (0.3 mL, 2.44 mmol), catalyst (0.005 mmol for **1**, 0.003 mmol for **2**, 0.01 mmol for **3**, 0.01 mmol for **4**) and 70% TBHP (0.754 mL, 4.88 mmol), acetonitrile (8 mL), temperature: 343 K, time: 12 h; [b] Average conversion of two runs based on GC results. The reaction mixture was analyzed twice, before and after treatment with PPh_3. No differences from each other were obtained. Carbon balance was also evaluated and found to be generally better than 93%. [c] Ethylbenzene conv (%) was defined as: Conv = $(n_{ap} + n_{ba} + n_{panol} + n_{other}) \times 100/n_{eb0}$; acetophenone selec (%) was defined as: Selec = $n_{ap} \times 100/(n_{ap} + n_{ba} + n_{panol} + n_{other})$ (n_{eb0}: the initial molar amount of ethylbenzene; eb = ethylbenzene; ap = acetophenone; ba = benzaldehyde; panol = 1-phenylethanol); the other products (mainly benzoic acid) have negligible yield in the reaction. [d] The yield of major product (acetophenone).

Based on the above-mentioned conditions, the conversions (and selectivities) for the oxidation of ethylbenzene are 27.6% (76.0%) for **1**, 22.4% (75.9%) for **2**, 51.1% (85.2%) for **3** and 44.3% (82.0%) for **4** as shown in Table 2.

To understand whether the different catalytic activities derive from the insoluble solid-state catalyst or from a small quantity of dissolved catalyst,[18] the amount of metal ions in the reaction filtrate was tested by atomic absorption spectra. No copper species (<0.1 ppm) was detected in the product solution, indicating that the oxidation process is truly catalyzed by the solid-state coordination polymers. Consistently, the solution was catalytically inactive after the catalysts were removed. We also evaluated the reusability of the catalysts, which show no significant loss in catalytic activity after the oxidation of ethylbenzene was recycled three times and its powder XRD patterns are almost unchanged before and after the reactions (Fig. 12). These results indicate that the catalytic activities for **1** to **4** are originated from the insoluble solid-state catalyst and thus are in the order of **3** ≈ **4** > **1** ≈ **2** for the oxidation of ethylbenzene.

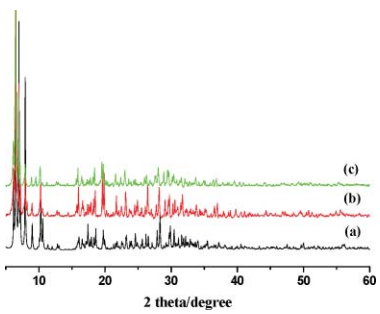

Fig. 12 XRPD patterns of **4** (a) simulation based on the single-crystal structure; (b) synthesized **4** at 298 K, (c) after reaction for 12 h at 343 K.

Since the catalytic activities of **1** to **4** for the oxidation reaction are originated from heterogeneous catalysts, the difference in their catalytic activities for **1** to **4** is thus related to the inherent property of their structures. Based on the structures of **1** to **4**, as well as the fact that the amount of $SiW_{12}O_{40}^{4-}$ was kept unchanged in the catalytic reaction for **1** to **4**, the main differences among the four

Table 3 Catalytic activities of **1** to **4** for the oxidation of styrene

Catalyst	*T* (K)	Conv (%)[a]	Selec (%)[b]	Selec (%)[c]
1	343	48.5	87.0	12.2
2	343	44.9	90.2	8.5
3	343	79.5	43.1	55.9
4	343	74.4	55.7	44.0
Blank	343	7.3	—	—

[a] Styrene (0.1 mL, 0.86 mmol), catalyst (0.005 mmol for **1**, 0.003 mmol for **2**, 0.01 mmol for **3**, 0.01 mmol for **4**) and 70% TBHP (0.2 mL, 1.29 mmol), acetonitrile (4 mL), temperature: 343 K, time: 10 h. [b] Benzaldehyde (ba) selec (%). [c] Styrene oxide selec (%).

coordination polymers are those of: (1) their dimension (from 0D to 3D for **1** to **4**); (2) the amount of 4,4′-Hbpy per mole $SiW_{12}O_{40}^{4-}$ (the amount of 4,4′-Hbpy per mole $SiW_{12}O_{40}^{4-}$ is 2 for **1**, 8/3 for **2** and 0 for **3** and **4** respectively); and (3) the amount of Cu(II) ion per mole of $SiW_{12}O_{40}^{4-}$ (the amount of Cu(II) ion for per mole of $SiW_{12}O_{40}^{4-}$ is 1 for **1**, 2/3 for **2**, 2 for **3** and 3 for **4**). Unambiguously, the difference in the dimensions for the four coordination polymers is not the key factor influencing their catalytic activities, since the coordination polymers are the heterogeneous catalysts and there is no pore existing in the coordination polymers. Similarly, the difference in the amount of Cu(II) ion in the four coordination polymers is not the key factor influencing their catalytic activities, because if the amount of Cu(II) ion plays a key contribution to the difference in catalytic activities of **1** to **4**, the catalytic activities for **1** to **4** would either be in the order of **4** > **3** > **1** > **2** when the amount of Cu(II) ion is positive for the catalytic reaction, or in the order of **4** < **3** < **1** < **2** when the amount of Cu(II) is negative for the catalytic reaction. Thus, the difference in the catalytic activities for the four coordination polymers is attributed to the amount of 4,4′-Hbpy.

To confirm it is the amount of 4,4′-Hbpy in the four coordination polymers that leads to the difference in their catalytic activities, $Na_4SiW_{12}O_{40}$ and $(NH_4)_4SiW_{12}O_{40}$ were respectively used as heterogeneous catalysts to perform the oxidation of ethylbenzene under the same reaction conditions as that described for **1** to **4**. Consistently, the conversion and selectivity for the oxidation of ethylbenzene are 27.5% and 76.4% for $Na_4SiW_{12}O_{40}$, significantly higher than those of 7.3% and 56.4% for $(NH_4)_4SiW_{12}O_{40}$.

Interestingly, in addition to the oxidation of ethylbenzene, the amount of 4,4′-Hbpy also significantly influences the oxidation of styrene (Scheme 2). As shown in Table 3, the conversion for the oxidation of styrene is 48.5% for **1**, 44.9% for **2**, 79.5% for **3** and 74.4% for **4**, while the selectivity for the oxidation of styrene to benzaldehyde and styrene oxide is 87.0% and 12.2% for **1**, 90.2% and 8.5% for **2**, 43.1% and 55.9% for **3**, and 55.7% and 44.0% for **4** respectively. This result indicates that the greater the amount of 4,4′-Hbpy, the less the conversion of the oxidation reaction, and the less the selectivity for the oxidation of styene to styene oxide, consistent with previous results that reveal the epoxide selectivity of styrene is acid sensitive,[19] due to the acid favoring epoxide ring opening.[19]

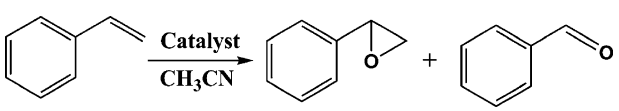

Scheme 2 Oxidation of styrene to benzaldehyde and styrene oxide.

Conclusion

In summary, we have successfully prepared four Keggin-based coordination polymers ranging from 0D dimer, 1D chain, 2D network to 3D framework based on similar modular building units under different pH conditions, revealing the crucial role of pH in the assembly of Keggin-based coordination polymers. Investigation of the catalytic activity of the four coordination polymers for the oxidation of ethylbenzene demonstrates that protonated 4,4′-bpy (4,4′-Hbpy) in the POMs-based coordination polymers significantly lowers their catalytic activities. Thus, the present work would aid our rational design and assembly of POM-based coordination polymers with higher catalytic activities.

Acknowledgements

We thank the NNSFC (Grant Nos. 20825103 and 20721001), the 973 Project from MSTC (Grant 2007CB815304) and the Natural Science Foundation of Fujian Province of China (Grant No. 2008J0010).

Notes and references

1 C. L. Hill (editor), *Chem. Rev.*, 1998, **98**(1), special issue on POMs.
2 C. L. Hill (editor), *J. Mol. Catal. A: Chem.*, 1996, **114**(1–3), special issue on POMs.
3 C. L. Hill and C. M. Prosser-McCartha, *Coord. Chem. Rev.*, 1995, **143**, 407; T. Okuhara, N. Mizuno and M. Misono, *Adv. Catal.*, 1996, **41**, 113; C. L. Hill, *J. Mol. Catal. A: Chem.*, 2007, **262**, 2.
4 N. Nojiri and M. Misono, *Appl. Catal., A*, 1993, **93**, 103; M. Misono, *Chem. Commun.*, 2001, 1141.
5 U. Kortz, S. S. Hamzeh and N. A. Nasser, *Chem.–Eur. J.*, 2003, **9**, 2945; J. M. Clemente-Juan, E. Coronado, A. Gaita-Arino, C. Gimenez-Saiz, H.-U. Gudel, A. Sieber, R. Bircher and H. Mutka, *Inorg. Chem.*, 2005, **44**, 3389; C. Zhang, R. C. Howell, Q.-H. Luo, H. L. Fieselmann, L. J. Todaro and L. C. Francesconi, *Inorg. Chem.*, 2005, **44**, 3569; S. C. Xiang, X. T. Wu, J. J. Zhang, R. B. Fu, S. M. Hu and X. D. Zhang, *J. Am. Chem. Soc.*, 2005, **127**, 16352; S. Nellutla, J. van Tol, N. S. Dalal, L.-H. Bi, U. Kortz, B. Keita, L. Nadjo, G. A. Khitrov and A. G. Marshall, *Inorg. Chem.*, 2005, **44**, 9795; H. Y An, E. B. Wang, D. R. Xiao, Y. G. Li, Z. M. Su and L. Xu, *Angew. Chem., Int. Ed.*, 2006, **45**, 904; D. L. Long, P. Kögerler, A. D. C. Parenty, J. Fielden and L. Cronin, *Angew. Chem., Int. Ed.*, 2006, **45**, 4798.
6 D Hagrman, P. J. Hagrman and J. Zubieta, *Angew. Chem., Int. Ed.*, 1999, **38**, 3165; I. Bar-Nahum and R. Neumann, *Chem. Commun.*, 2003, 2690; Y. Kikukawa, S. Yamaguchi, K. Tsuchida, Y. Nakagawa, K. Uehara, K. Yamaguchi and N. Mizuno, *J. Am. Chem. Soc.*, 2008, **130**, 5472.
7 V. Shivaiah, M. Nagaraju and S. K. Das, *Inorg. Chem.*, 2003, **42**, 6604; J. Lu, E. H. Shen, M. Yuan, Y. G. Li, E. B. Wang, C. W. Hu, L. Xu and J. Peng, *Inorg. Chem.*, 2003, **42**, 6956; H. Zhang, L. Y. Duan, Y. Lan, E. B. Wang and C. W. Hu, *Inorg. Chem.*, 2003, **42**, 8053; Y. Ishii, Y. Takenaka and K. Konishi, *Angew. Chem., Int. Ed.*, 2004, **43**, 2702.
8 P. J. Hagrman, D. Hagrman and J. Zubieta, *Angew. Chem., Int. Ed.*, 1999, **38**, 2639; C. M. Liu, D. Q. Zhang, M. Xiong and D. B. Zhu, *Chem. Commun.*, 2002, 1416; A. Dolbecq, P. Mialane, L. Lisnard, J. Marrot and F. Sécheresse, *Chem.–Eur. J.*, 2003, **9**, 2914; B. Z. Lin, Y. M. Chen and P. D. Liu, *Dalton Trans.*, 2003, 2474; C. Lei, J. G. Mao, Y. Q. Sun and J. L. Song, *Inorg. Chem.*, 2004, **43**, 1964.
9 M. T. Pope and A. Müller, *Angew. Chem., Int. Ed. Engl.*, 1991, **30**, 34; M. Sadakane, M. H. Dickman and M. T. Pope, *Angew. Chem., Int. Ed.*, 2000, **39**, 2914; E. Burkholder, V. Golub, C. J. O'Connor and J. Zubieta, *Chem. Commun.*, 2003, 2128.
10 E. F. Wilson, H. Abbas, B. J. Duncombe, C. Streb, D.-L. Long and L. Cronin, *J. Am. Chem. Soc.*, 2008, **130**, 13876; J. Macht, M. J. Janik, M. Neurock and E. Iglesia, *J. Am. Chem. Soc.*, 2008, **130**, 10369; M. A. AlDamen, J. M. Clemente-Juan, E. Coronado, C. Martí-Gastaldo and A. Gaita-Ariño, *J. Am. Chem. Soc.*, 2008, **130**, 8874; S.-T. Zheng, J Zhang and G.-Y. Yang, *Angew. Chem., Int. Ed.*, 2008, **47**, 3909;

D. L. Long, Y. F. Song, E. F. Wilson, P. Kogerler, S. X. Guo, A. M. Bond, J. S. J. Hargreaves and L. Cronin, *Angew. Chem., Int. Ed.*, 2008, **47**, 4384.
11 C.-Y. Sun, S.-X. Liu, D.-D. Liang, K.-Z. Shao, Y.-H Ren and Z.-M Su, *J. Am. Chem. Soc.*, 2009, **131**, 1883; V. Mirkhani, M. Moghadam, S. Tangestaninejad, I. Mohammadpoor- Baltork and N. Rasouli, *Catal. Commun.*, 2008, **9**, 2411; N. M. Okun, T. M. Anderson and C. L. Hill, *J. Am. Chem. Soc.*, 2003, **125**, 3194; B. Botar, Y. V. Geletii, P. Kögerler, D. G. Musaev, K. Morokuma, I. A. Weinstock and C. L. Hill, *J. Am. Chem. Soc.*, 2006, **128**, 11268; Y. Nishiyama, Y. Nakagawa and N. Mizuno, *Angew. Chem., Int. Ed.*, 2001, **40**, 3639.
12 N. M. Okun, T. M. Anderson, K. I. Hardcastle and C. L. Hill, *Inorg. Chem.*, 2003, **42**, 6610; Y. V. Geletii, B. Botar, P. Kögerler, D. A. Hillesheim, D. G. Musaev and C. L. Hill, *Angew. Chem., Int. Ed.*, 2008, **47**, 3896; J. W. Han and C. L. Hill, *J. Am. Chem. Soc.*, 2007, **129**, 15094; Z. Luo, P. Kögerler, R. Cao and C. L. Hill, *Inorg. Chem.*, 2009, **48**, 7812.
13 P.-Q. Zheng, Y.-P. Ren, L.-S. Long, R.-B. Huang and L.-S. Zheng, *Inorg. Chem.*, 2005, **44**, 1190; Y.-P. Ren, X.-J. Kong, L.-S. Long, R.-B Huang and L.-S. Zheng, *Cryst. Growth Des.*, 2006, **6**, 572.
14 X.-J. Kong, Y.-P Ren, Y.-X. Long, P.-Q. Zheng, L.-S. Long, R.-B. Huang and L.-S. Zheng, *Inorg. Chem.*, 2006, **45**, 10702; Y.-P. Ren, X.-J. Kong, X.-Y. Hu, M. Sun, L.-S. Long, R.-B Huang and L.-S. Zheng, *Inorg. Chem.*, 2006, **45**, 4016.
15 G. M. Sheldrick, *SADABS, version 2.05*University of Göttingen, Göttingen, Germany.
16 *SHELXTL 6.10,*Bruker Analytical Instrumentation, Madison, WI, 2000.
17 optimized reaction condition: ethylbenzene (0.3 mL, 2.44 mmol), 70% TBHP (0.754 mL, 4.88 mmol), acetonitrile (8 mL), reaction temperature: 343 K, reaction time: 12 h.
18 J. T. Rhule, W. A. Neiwert, K. I. Hardcastle, B. T. Do and C. L. Hill, *J. Am. Chem. Soc.*, 2001, **123**, 12101.
19 P. Liu, C. H. Wang and C. Li, *J. Catal.*, 2009, **262**, 159; P. Liu, H. Wang, Z. C. Feng, P. L. Ying and C. Li, *J. Catal.*, 2008, **256**, 345; W. C. Zhan, Y. L. Guo, Y. Q. Wang, Y. Guo, X. H. Liu, Y. S. Wang, Z. G. Zhang and G. Z. Lu, *J. Phys. Chem. C*, 2009, **113**, 7181.